ChemComm

COMMUNICATION

View Article Online
View Journal | View Issue

Cite this: *Chem. Commun.*, 2024, **60**, 3818

Received 18th January 2024,
Accepted 7th March 2024

DOI: 10.1039/d4cc00268g

rsc.li/chemcomm

Synthesis, structure and stereodynamics of atropisomeric *N*-chloroamides†

Aaron D. G. Campbell,[a] Natalie J. Roper,[a] Paul G. Waddell,[a] Corinne Wills,[a] Casey M. Dixon,[a] Ross M. Denton,[b] Kristaps Ermanis*[b] and Roly J. Armstrong*[a]

Atropisomeric *N*-chloroamides were efficiently accessed by electrophilic halogenation of *ortho*-substituted secondary anilides. The stereodynamics of atropisomerism in these novel scaffolds was interrogated by detailed experimental and computational studies, revealing that racemization is correlated with amide isomerization. The stereoelectronic nature of the amide was shown to significantly influence racemization rates, with potentially important implications for other C–N atropisomeric scaffolds.

Atropisomers are valuable molecules with powerful applications in catalysis, materials science and medicines.[1] The archetypal examples are axially chiral biaryls, whose stereoisomerism derives from restricted rotation about a C–C bond (Scheme 1A).[2] The mechanism of racemization in biaryls is well understood and the configurational stability of new materials can be straightforwardly predicted by computational simulation.[3] Recently, a growing number of elegant reports have emerged involving atropisomerism about C–N bonds, perhaps most notably in *ortho*-substituted anilides, which can exhibit robust configurational stability and have emerging potential in medicines (*e.g.* the drug telenzepine) and agriscience (*e.g.* the herbicide metolachlor).[4] However, in contrast to biaryls, atropisomerism in anilides is complicated by the possibility of rotation about multiple bonds. Although several studies have interrogated the impact of structural modifications on the configurational stability of anilides,[5,6] it is not established whether racemization occurs *via* direct Ar–N bond rotation or in correlation with rotation about the N–CO bond as reported by Clayden and co-workers for C–C atropisomeric benzamides.[7] Consequently, it is extremely challenging to predict the racemization rates of new compounds *a priori*. Understanding the stereodynamic processes underpinning racemization could significantly streamline the identification of new C–N atropisomeric materials.

Exemplifying these challenges, we recently questioned whether it might be possible to access unique *N*-haloamide atropisomers **2** *via* electrophilic chlorination of secondary anilides **1** (Scheme 1B). Given the ubiquitous use of *N*-haloamide reagents in organic synthesis, accessing the first examples of axially chiral analogues would be of significant interest.[8] However, given the unprecedented nature of these scaffolds, it was not clear whether they would display atropisomeric behaviour. Here we report our preliminary results, which reveal that axially chiral *N*-chloroamides can be efficiently synthesised and display high levels of chemical and configurational stability ($t_{1/2}^{rac}$ up to 12 days). These novel atropisomeric scaffolds have provided an ideal basis to explore the

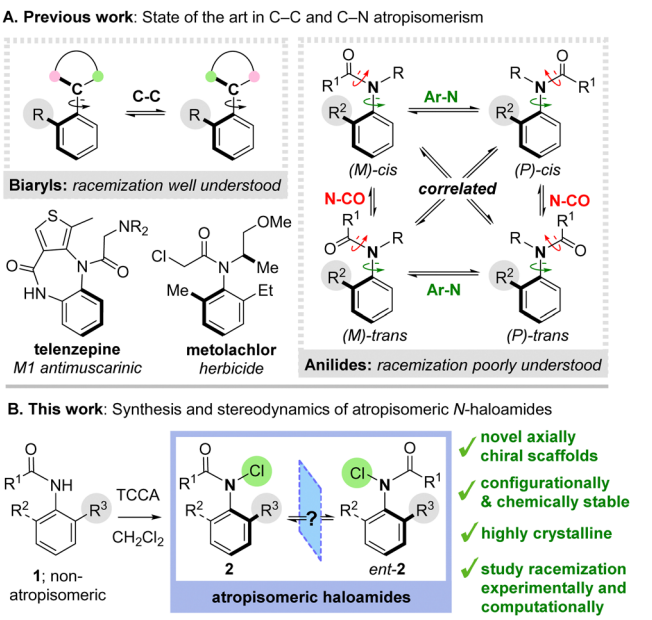

Scheme 1 Potential and challenges associated with atropisomerism in anilides, and expansion to atropisomeric *N*-haloamides.

[a] *Chemistry – School of Natural and Environmental Sciences, Newcastle University, Newcastle Upon Tyne, NE1 7RU, UK. E-mail: roly.armstrong@newcastle.ac.uk*
[b] *School of Chemistry, University Park, Nottingham, UK. E-mail: kristaps.ermanis@nottingham.ac.uk*

† Electronic supplementary information (ESI) available: Detailed experimental procedures and characterization data for new compounds. CCDC 2307639–2307647. For ESI and crystallographic data in CIF or other electronic format see DOI: https://doi.org/10.1039/d4cc00268g

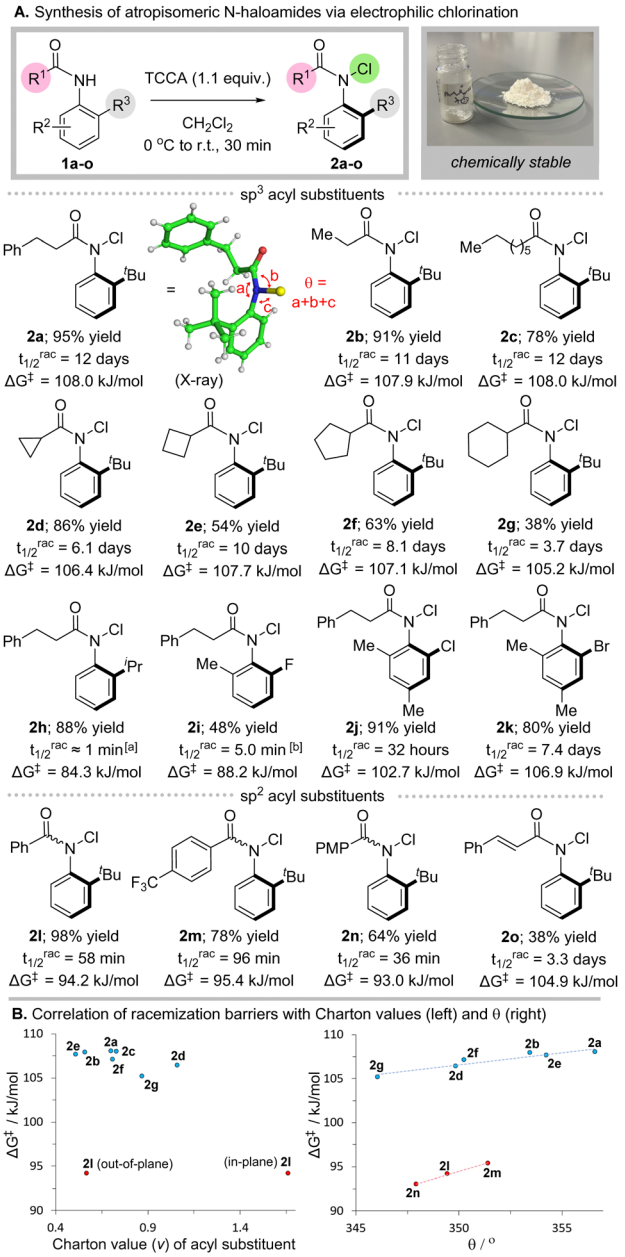

Scheme 2 Synthesis of *N*-chloroamides and experiments to probe atropisomerism. Yields refer to isolated material after column chromatography. Depictions of absolute stereochemistry are arbitrary. [a] $t_{1/2}^{rac}$ estimated at 20 °C based on $\Delta G^{\ddagger}$ measured at 5 °C by dynamic HPLC analysis. [b] Determined by dynamic HPLC analysis at 20 °C.[9,10]

stereodynamics of anilide racemization through experimental and computational studies, providing insight into the degree of correlation with N–CO rotation.

We commenced our study by exploring the electrophilic chlorination of secondary anilides **1** (Scheme 2A). We were pleased to find that treatment with a slight excess of trichloroisocyanuric acid (TCCA) in dichloromethane led to efficient formation of the corresponding *N*-chloroamides **2**, with no evidence of competing aromatic chlorination. This synthetic approach was applied to prepare a library of *ortho*-substituted chloroamides bearing various sp^3 or sp^2 acyl substituents (**2a–o**). Notably, these *N*-haloamides displayed excellent chemical stability – they could be isolated by routine aqueous workup and column chromatography, characterized using standard spectroscopic methods, and stored at −18 °C for several months without decomposition.

With an efficient synthesis of *N*-chloroamides established, we investigated their configurational stability. HPLC analysis of **2a** on a chiral stationary phase revealed two baseline-separated peaks, consistent with a pair of enantiomers which do not interconvert on the timescale of the HPLC experiment. An enantioenriched sample (obtained by semi-preparative HPLC) was allowed to stand at room temperature and its enantiomeric excess was monitored over time.[9] We calculated a racemization half-life ($t_{1/2}^{rac}$) of 12 days corresponding to a Gibbs activation energy of enantiomerization ($\Delta G^{\ddagger}$) of 108.0 kJ mol^{-1} (see ESI†). Similar analysis was performed on *N*-chloroamides **2a–o** and the resulting values of $t_{1/2}^{rac}$ and $\Delta G^{\ddagger}$ are shown in Scheme 2A.[9] Relatively robust configurational stability was observed across analogues bearing various aliphatic acyl substituents (**2a–g**), but chloroamide **2h** bearing a smaller *ortho*-isopropyl group racemized rapidly.[9,10] We also explored anilides **2i–k** bearing two *ortho* substituents. Robust configurational stability was observed for brominated analogue **2k**, but chlorinated and fluorinated analogues **2j** and **2i** underwent comparatively rapid racemization. This is interesting given that C–N atropisomeric sulfonamides derived from 2-chloro-4,6-dimethylaniline have been reported to display higher configurational stability than analogues bearing a single *ortho* ^{t}Bu-substituent.[11] Moreover, examples bearing an aromatic acyl group (**2l–n**) also racemized extremely rapidly ($t_{1/2}^{rac} < 2$ h). To investigate this observation further, we plotted the experimentally determined values for $\Delta G^{\ddagger}$ against the Charton steric parameters (ν) associated with the various acyl substituents (Scheme 2B, left).[12] This analysis is complicated by the fact that two values of ν are available for the Ph group (out of plane = 0.57; in plane = 1.66), but even for structurally similar aliphatic analogues **2a–g** a poor correlation was observed. Shi and co-workers have postulated that electronic effects have an effect on the racemization rate of anilides bearing aromatic acyl substituents, and we speculated that the ability of the amide to deplanarise during racemization may also be playing an important role here.[5a] We were fortunate to be able to obtain crystals of **2a** suitable for single crystal X-ray diffraction allowing us to probe the structure of the amide in the solid state (Scheme 2A). In particular, the planarity of the amide nitrogen atom was studied by evaluating the angle parameter θ, corresponding to the sum of the three valence angles about the nitrogen atom.[13] For amide **2a**, such analysis revealed a value of θ = 356.6° close to the ideal value of 360° expected from a completely trigonal arrangement. We also obtained X-ray crystal structures of several other *N*-chloroamides depicted in Scheme 2 (**2a–b**, **d–g**, **l–n**), many of which displayed significantly more distorted nitrogen atoms (*e.g.* **2g**, R^1 = Cy, θ = 346.1°). Interestingly, when θ was plotted against $\Delta G^{\ddagger}$, for aliphatic examples **2a–g** a positive correlation (R^2 = 0.90) was observed (Scheme 2B, right). A similar trend was observed for examples **2l–n** bearing aromatic amide substituents. This data must be interpreted with some caution, but may suggest that amides possessing a more conformationally distorted ground state are able to racemize more rapidly. However this effect does not explain the

significantly reduced configurational stability of examples containing aliphatic *vs.* aromatic acyl substituents (*e.g.*, anilides **2d** and **2l** possess similar values of θ, but **2l** racemizes two orders of magnitude more rapidly).

A similar effect has been reported by Curran and co-workers in atropisomeric *N*-methyl anilides, with benzoylated analogues racemizing significantly faster than examples bearing aliphatic acyl substituents.[5e] In this case, it was also noted that benzoylated analogues displayed a higher preference for the *trans*-amide isomer. In line with this observation, we noticed that the X-ray structures of aliphatic chloroanilides (**2a–b**, **d–g**) possessed a *cis*-configured amide, but in contrast, the structures of aromatic anilides **2l–n** featured a *trans*-amide geometry.[14] To probe if similar behaviour is observed in solution, we analyzed **2a** by ^{1}H NMR in $CDCl_3$ at 298 K and observed a single set of broad peaks (Scheme 3A). Upon cooling to 233 K, the spectrum resolved to reveal two well-defined species present in a 93 : 7 mixture, which were characterized as the *cis*- and *trans*-amide isomers respectively on the basis of NOE-analysis. Strong EXSY correlations were also observed between geometrical isomers, indicating relatively rapid exchange even at 273 K (see ESI† for details). Phenyl-substituted amide **2l** also exhibited a single set of broad peaks at room temperature, but upon cooling to 218 K resolved into two geometrical isomers with a slight preference for the *trans*-isomer (Scheme 3B). From this data, we concluded: (i) geometrical isomerization of the amide is extremely fast compared with racemization; (ii) the ratio of geometrical isomers is governed by thermodynamics and not established during chlorination; (iii) the nature of the acyl substituent exerts a significant influence on the position of equilibrium, with aliphatic groups resulting in a near exclusive preference for the *cis*-geometry but aromatic groups leading to a higher equilibrium population of the *trans*-isomer.

To gain insight into how these factors relate to configurational stability, DFT modelling studies were conducted (ωB97M-V[15]/def2-QZVPP[16]/SMD(*n*-hexane)[17]//PBE0-D3[18]/def2-TZVP/SMD(*n*-hexane), see ESI† for full details). For a representative chloroamide **2b** (Scheme 4A), our analysis suggested that the lowest energy racemization pathway occurs *via* a Clayden-type correlated mechanism, in which Ar–N bond rotation is geared with N–CO isomerization (calculated $\Delta G^{\ddagger}$ = 117.2 kJ mol^{-1}). We were unable to find any energetically feasible processes involving direct Ar–N bond rotation (without amide isomerization) from either *cis*- or *trans*-amide rotamers. (*P*)-*trans*-**2b** formed in this correlated isomerization was calculated to be destabilised with respect to the starting material by 2.1 kJ mol^{-1}, but can isomerize to the thermodynamically favoured *cis*-amide *via* a facile N–CO bond rotation ($\Delta G^{\ddagger}$ = 58.7 kJ mol^{-1}). This is broadly consistent with our experimental observations for **2b**, namely a *cis*/*trans* ratio of ∼9 : 1 observed at 263 K by ^{1}H NMR, and rapid exchange of amide rotamers at room temperature. Equivalent analyses of chloroamides **2d**, **2l** and **2n** suggested a similar racemization mechanism *via* correlated Ar–N and N–CO rotation (Scheme 4B). The calculated values of $\Delta G^{\ddagger}$ were somewhat higher than those determined experimentally, but reproduced the experimentally observed trend with good fidelity (**2b** > **2d** ≫ **2l** > **2n**). For all four examples, the computed racemization pathway involves a significant reduction in N–CO bond order from 1.13 to 0.95 on average, accompanied by a smaller increase in Ar–N bond order in the transition state (TS) from 0.85 to 1.01 on average. In all cases there was also a decrease in the planarity of the N atom in the TS compared to the ground state. This is consistent with deconjugation of the nitrogen lone pair from the amide in order to partially re-conjugate with the *ortho*-substituted aromatic ring and is also in line with our experimental result that increased distortion about the nitrogen atom in the ground state (*i.e.* weakening of the amide bond) correlates with more facile racemization (also replicated computationally, see ESI†). In line with the experimental data, for **2l** and **2n** our calculations also show that the *cis*-amide is destabilised relative to the *trans*-isomer by 3.4 and 4.8 kJ mol^{-1}, respectively.

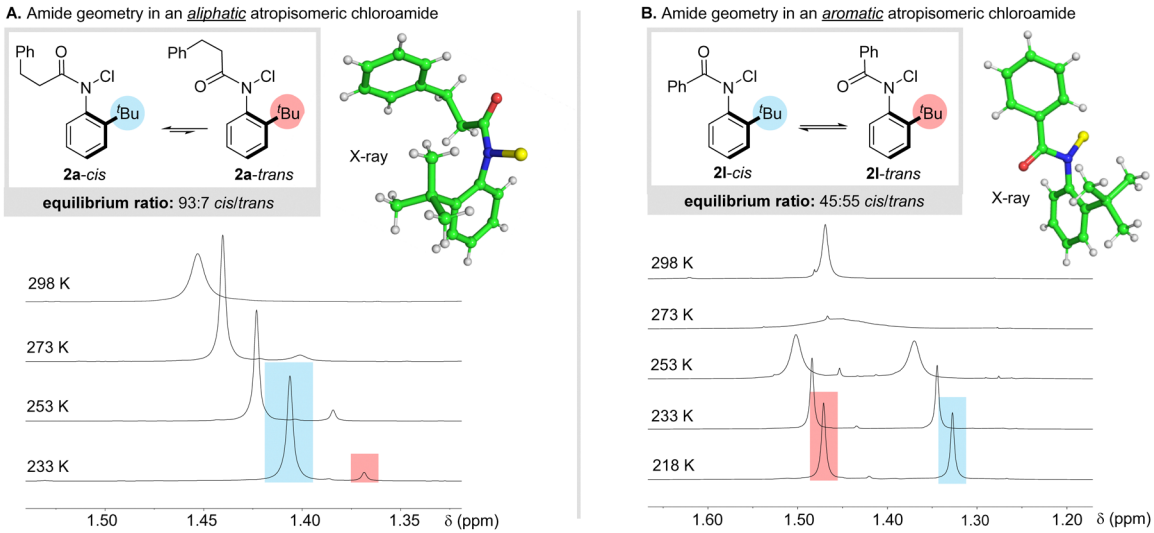

Scheme 3 Conformational analysis of aromatic and aliphatic *N*-chloroamides **2a** and **2l** by variable-temperature ^{1}H NMR spectroscopy and X-ray crystallography. Stack plots show the *tert*-butyl region, with spectra offset for clarity (full spectra are included in the ESI†).

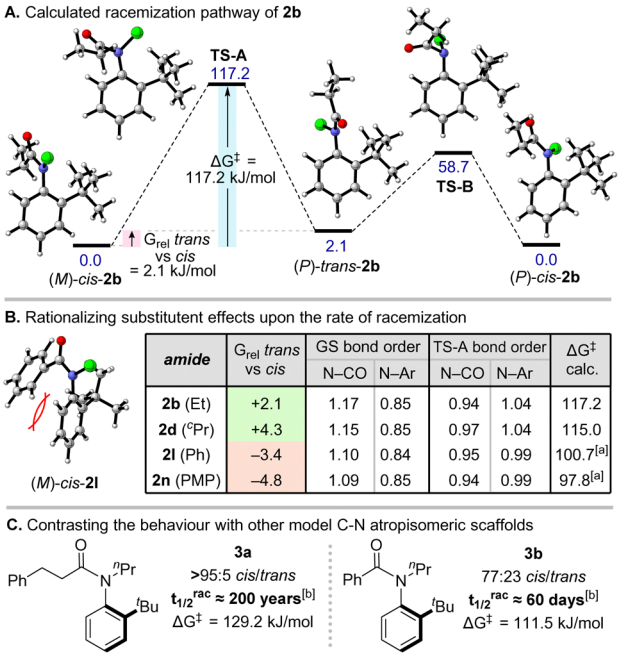

Scheme 4 Computational analysis of chloroanilide racemization and comparison with model scaffolds bearing non-halogen *N*-substituents. Calculations were carried out at the PBE0-D3/def2-tzvp/SMD(*n*-hexane)//wB97M-V/def2-QZVPP/SMD(*n*-hexane) level. Free energies are reported in kJ mol^{-1}. [a] $\Delta G^{\ddagger}$ calculated from lowest energy *trans*-amide. [b] $t_{1/2}^{rac}$ for **3a** and **3b** estimated at 20 °C based on $\Delta G^{\ddagger}$ measured at elevated temperature in 2,2,4-trimethylpentane (see ESI†).

This is likely a consequence of an unfavourable interaction in the *cis*-amide between the benzoyl group and the N–Ar group. Interestingly, in all four compounds the *cis* isomer features a stronger amide bond than in the *trans* (bond order 1.17 *vs.* 1.11 on average). Overall, we believe that the experimentally and computationally observed ground state destabilization in benzoylated analogues may explain their significantly more facile racemization.

Finally, to establish the generality of our conclusions, we prepared compounds **3a–b** bearing an *N*-propyl group (Scheme 4C). In line with our study, hydrocinnamoyl analogue **3a** was observed as a single *cis*-amide (>95 : 5 *cis*/*trans*) with a high racemization barrier ($t_{1/2}^{rac} \approx 200$ years). In contrast, for benzoyl analogue **3b**, an appreciable amount of *trans*-amide was observed (77 : 23 *cis*/*trans*) accompanied by a dramatic reduction in configurational stability ($t_{1/2}^{rac} \approx 60$ days). Taken together with the similar results reported by Curran and co-workers, these results imply that the stereodynamic processes described here may apply more generally to other C–N atropisomers.

In summary, we have developed the first synthesis of atropisomeric *N*-haloamides. Experimental and computational studies established that stereoelectronics of the amide play a key role in dictating the racemization rate. Computational studies suggest racemization occurs *via* correlated rotation about the Ar–N and N–CO bonds, which may have important implications for the wider field of C–N atropisomerism. Research in our laboratory is currently ongoing to develop asymmetric syntheses of *N*-chloroamides and harness them in asymmetric halogenation processes.

We gratefully acknowledge financial support from EPSRC (EP/S022791/1), Newcastle University, the Royal Society (RGS\R1\221162) and the Bill and Milica Beck PhD Endowment Fund. We also thank Vertex Pharmaceuticals for generous provision of equipment. Calculations were performed using the Sulis Tier 2 HPC platform hosted by the Scientific Computing Research Technology Platform at the University of Warwick. Sulis is funded by EPSRC Grant EP/T022108/1 and the HPC Midlands+ consortium.

Conflicts of interest

There are no conflicts to declare.

Notes and references

1 J. K. Cheng, S.-H. Xiang, S. Li, L. Ye and B. Tan, *Chem. Rev.*, 2021, **121**, 4805–4902.
2 J. Wencel-Delord, A. Panossian, F. R. Leroux and F. Colobert, *Chem. Soc. Rev.*, 2015, **44**, 3418–3430.
3 S. R. LaPlante, P. J. Edwards, L. D. Fader, A. Jakalian and O. Hucke, *ChemMedChem*, 2011, **6**, 505–513.
4 (*a*) J. S. Sweet and P. C. Knipe, *Synthesis*, 2022, 2119–2132; (*b*) Y.-J. Wu, G. Liao and B.-F. Shi, *Green Synth. Catal.*, 2022, **3**, 117–136; (*c*) P. Rodríguez-Salamanca, R. Fernández, V. Hornillos and J. M. Lassaletta, *Chem. – Eur. J.*, 2022, **28**, e202104442; (*d*) G.-J. Mei, W. L. Koay, C.-Y. Guan and Y. Lu, *Chemistry*, 2022, **8**, 1855–1893; (*e*) A. D. G. Campbell and R. J. Armstrong, *Synthesis*, 2023, 2427–2438.
5 (*a*) Q.-J. Yao, P.-P. Xie, Y.-J. Wu, Y.-L. Feng, M.-Y. Teng, X. Hong and B.-F. Shi, *J. Am. Chem. Soc.*, 2020, **142**, 18266–18276; (*b*) N. Suzumura, M. Kageyama, D. Kamimura, T. Inagaki, Y. Dobashi, H. Hasegawa, H. Fukaya and O. Kitagawa, *Tetrahedron Lett.*, 2012, **53**, 4332–4336; (*c*) K. Kondo, H. Fujita, T. Suzuki and Y. Murakami, *Tetrahedron Lett.*, 1999, **40**, 5577–5580; (*d*) K. Kondo, T. Iida, H. Fujita, T. Suzuki, K. Yamaguchi and Y. Murakami, *Tetrahedron*, 2000, **56**, 8883–8891; (*e*) D. P. Curran, G. R. Hale, S. J. Geib, A. Balog, Q. B. Cass, A. L. G. Degani, M. Z. Hernandes and L. C. G. Freitas, *Tetrahedron: Asymmetry*, 1997, **8**, 3955–3975.
6 For related studies on amines, see: (*a*) R. Costil, A. J. Sterling, F. Duarte and J. Clayden, *Angew. Chem., Int. Ed.*, 2020, **59**, 18670–18678; (*b*) T. Kawabata, C. Jiang, K. Hayashi, K. Tsubaki, T. Yoshimura, S. Majumdar, T. Sasamori and N. Tokitoh, *J. Am. Chem. Soc.*, 2009, **131**, 54–55; (*c*) Y. Iwasaki, R. Morisawa, S. Yokojima, H. Hasegawa, C. Roussel, N. Vanthuyne, E. Caytan and O. Kitagawa, *Chem. – Eur. J.*, 2018, **24**, 4453–4458; G. Furukawa, T. Shirai, Y. Homma, E. Caytan, N. Vanthuyne, D. Farran, C. Roussel and O. Kitagawa, *J. Org. Chem.*, 2020, **85**, 5109–5113; (*d*) D. Homma, S. Taketani, T. Shirai, E. Caytan, C. Roussel, J. Elguero, I. Alkorta and O. Kitagawa, *J. Org. Chem.*, 2022, **87**, 8118–8125.
7 (*a*) J. Clayden and J. H. Pink, *Angew. Chem., Int. Ed.*, 1998, **37**, 1937–1939; (*b*) R. A. Bragg, J. Clayden, G. A. Morris and J. H. Pink, *Chem. – Eur. J.*, 2002, **8**, 1279–1289; (*c*) D. R. Hirsch, A. J. Metrano, E. A. Stone, G. Storch, S. J. Miller and R. P. Murelli, *Org. Lett.*, 2019, **21**, 2412–2415.
8 W. M. Gołębiewski and M. Gucma, *Synthesis*, 2007, 3599–3619.
9 J.-P. Heeb, J. Clayden, M. D. Smith and R. J. Armstrong, *Nat. Protoc.*, 2023, **18**, 2745–2771.
10 O. Trapp, *Chirality*, 2006, **18**, 489–497.
11 Z. Gao, C.-X. Yan, J. Qian, H. Yang, P. Zhou, J. Zhang and G. Jiang, *ACS Catal.*, 2021, **11**, 6931–6938.
12 (*a*) M. Charton, *J. Am. Chem. Soc.*, 1975, **97**, 1552–1556; (*b*) M. Charton, *J. Org. Chem.*, 1976, **41**, 2217–2220.
13 Y. Otani, O. Nagae, Y. Naruse, S. Inagaki, M. Ohno, K. Yamaguchi, G. Yamamoto, M. Uchiyama and T. Ohwada, *J. Am. Chem. Soc.*, 2003, **125**, 15191–15199.
14 G. J. Pros and A. J. Bloomfield, *J. Phys. Chem. A*, 2019, **123**, 7609–7618.
15 N. Mardirossian and M. Head-Gordon, *J. Chem. Phys.*, 2016, **144**, 214110.
16 (*a*) F. Weigend and R. Ahlrichs, *Phys. Chem. Chem. Phys.*, 2005, **7**, 3297–3305; (*b*) F. Weigend, *Phys. Chem. Chem. Phys.*, 2006, **8**, 1057–1065.
17 A. V. Marenich, C. J. Cramer and D. G. Truhlar, *J. Phys. Chem. B*, 2009, **113**, 6378–6396.
18 C. Adamo and V. Barone, *J. Chem. Phys.*, 1999, **110**, 6158–6169.